

Article

Effects of Sex and 17 β -Estradiol on Cardiac Fibroblast Morphology and Signaling Activities *in vitro*

Kelsey Watts¹, Will Richardson^{1,*}¹ Department of Bioengineering, Clemson University, Clemson, SC* Correspondence: wricha4@clemson.edu

Abstract: Several studies have demonstrated estrogen's cardioprotective abilities in decreasing the fibrotic response of cardiac fibroblasts (CFs). However, the majority of these studies are not sex-specific, and those at the cellular level utilize tissue culture plastic, a substrate that has a stiffness much higher than physiological conditions. Understanding the intrinsic differences between male and female CFs under more physiologically "healthy" conditions will help to elucidate the divergences in their complex signaling networks. We aimed to do this by conducting sex-disaggregated analysis of changes in cellular morphology and relative concentrations of profibrotic signaling proteins in CFs cultured on 8kPa stiffness plates with and without 17- β estradiol (E2). Cyclic immunofluorescent analysis indicated that there is a negligible change in cellular morphology due to sex and E2 treatment and that the differences between male and female CFs are occurring at a biochemical rather than structural level. Several proteins corresponding to profibrotic activity had various sex-specific responses with and without E2 treatment. Single-cell correlation analysis exhibited varied protein-protein interaction across experimental conditions. These findings demonstrate the need for further research into the dimorphisms of male and female CFs to develop better tailored, sex-informed prevention and treatment interventions of cardiac fibrosis.

Keywords: cardiac fibroblasts, sex-specific, estrogen, fibrosis, heart failure

1. Introduction

The prevalence of heart failure (HF) continues to rise, currently afflicting over 6.2 million Americans in roughly equal proportions among men and women[1,2]. What is not equal is the diagnosis, prognosis, treatment, and overall understanding of HF on the basis of biological sex[2–5]. Female data are underrepresented in animal studies and clinical trials, so recommended treatment is not sex-specific, and adverse drug reactions occur at double the rate in women than men[4]. Interestingly, premenopausal women have a relative protection against HF compared to age-matched men which subsides once they have undergone menopause[2,6]. This phenomenon has been studied extensively and is largely thought to be because of the ovarian hormone estrogen[3,4,7]. Hormone replacement therapy (HRT) to maintain estrogen levels in postmenopausal women was even considered cardioprotective for several decades[8,9]. However, following randomized clinical studies, HRT was shown to have overall adverse trends, increasing the risk of stroke, breast cancer, and even heart attack in postmenopausal women, and is not recommended for long-term use or as a preventive measure for cardiovascular diseases[6,8].

Although complete HRT is not a viable option to treat or prevent cardiac pathologies, 17- β estradiol (E2) has exhibited promise in reducing cardiac fibrosis - an accumulation of collagens and other extracellular matrix components, reducing pump and electrical function[7,10–12]. After an initial myocardial infarction, a fibrotic response is necessary to maintain structural stability but can continue uncontrolled resulting in chronic HF[13]. There are currently no FDA-approved therapeutics to specifically target and control cardiac fibrosis[13]. In many *in vitro* studies, E2 treatment has been linked to a decreased fibrotic response of cardiac fibroblasts (CF) indicating its potential as a therapeutic[10–

12,14–16]. It is important to note, many of these studies were done with neonatal rat CFs, pooling male and female cells together, so sex-specific effects of estrogen treatment were, for the most part, not investigated. Understanding how estrogen is interacting with male and female cells at a molecular level is imperative to being able to leverage estrogen's therapeutic effects while minimizing potential adverse responses.

Additionally, the few studies that do use sex-disaggregated analysis at the cellular level are nearly all using tissue culture plastic (TCP) as the platform for experiments. TCP has a stiffness that is magnitudes higher than physiologic conditions, even a fibrotic environment. CFs are extremely sensitive to their microenvironment and when cultured on stiff substrates, many proteins become activated due to mechanotransduction pathways that can make cells profibrotic[17–19]. Understanding the intrinsic differences between male and female CFs under physiologically “healthy” conditions is a first necessary step to being able to understand the divergence of their intricate signaling pathways related to fibrosis.

Expanding our knowledge of how estrogen interacts with both male and female CFs could help elucidate new potential treatment options for cardiac fibrosis which leverage estrogen's cardioprotective properties while mitigating its harmful effects. In this study, we used cyclic immunofluorescence to investigate potential morphological changes, cellular localization, and activity levels of 12 proteins known to be heavily involved in estrogen and/or profibrotic signaling within CFs. This allowed for a sex-disaggregated analysis of not only each individual protein's response to estrogen, but also single-cell cross-correlation analysis which could uncover protein to protein crosstalk that could be potential sites to target for regulation of cardiac fibrosis.

2. Materials and Methods

2.1 Cell Isolation and Culture

Age-matched adult Sprague Dawley rats (n=8 male and n=8 female) were euthanized and hearts were removed and collected in Krebs-Henseleit buffer (Sigma, St. Louis, MO). All procedures were performed with approval from Clemson University's Institutional Animal Care and Use Committee. Ventricles were minced and digested to isolate CFs according to previously reported protocols[20,21]. Liberase TM (Roche, Indianapolis, IN) was used in each of the six successive enzymatic digestions at 37 C. Supernatants from each digestion were collected and centrifuged at 300 g and 4 C, and resuspended in Dulbecco's Modified Eagle's Medium (DMEM, Sigma) containing 10% fetal bovine serum (FBS, Atlanta Biologicals, Flowery Branch, GA), 100 U/mL penicillin G, 100 µg/mL streptomycin, and 1 ng/mL amphotericin B (all Sigma). Following isolation cells were plated in T-25 culture flasks and incubated at 37 C and 5% CO₂ for 4 h, after which media was changed and continued to be changed every 72 h until use in experiments.

2.2 Collagen Coated Culture Plates

Prior to cell plating, 8 kPa 24-well CytoSoft® plates (Advanced BioMatrix, San Diego, CA) were coated with Telocol-3 bovine collagen (Advanced BioMatrix). Collagen solution was made at a 1:30 ratio of Telocol-3 in Phosphate Buffered Saline (PBS, Sigma). 1 mL of solution was pipetted into each of the 24 wells and allowed to polymerize at room temperature for 1 h. Excess solution was removed and the wells were washed with PBS twice.

2.3 Estrogen Treatment

Male and female CFs were passaged one time with 0.25% trypsin (Fisher) at a 1:3 dilution before use in experiments. Once the CFs had reached ~75% confluence after the first passage, DMEM containing 10% FBS was removed and flasks were washed with PBS. A 24 h serum starvation was started with phenol-free DMEM (Fisher) + 2 mM L-glutamine (Fisher) and 2.5% charcoal-stripped FBS (GE Health, Chicago, IL) incubated at 37 C and 5% CO₂. After 24 h, CFs were passaged and plated onto the CytoSoft® plates at 10,000 cells/well. CFs were divided into 4 experimental groups across two conditions: male vs.

female and with or without 17- β Estradiol (E2, Sigma). The 24-well plates allowed for three technical replicates (wells) of each biological replicate per experimental condition. All wells were filled with 1 mL of phenol-free DMEM + 2 mM L-glutamine and 10% charcoal stripped FBS. E2 was dissolved in ethanol at 10 mM and 10 nM of E2 was added to wells designated for E2 treatment. An ethanol vehicle control of 10 nM was used as a control for all non E2 treated wells. Plates were incubated at 37 C and 5% CO₂ for 24 h. Following incubation, all wells were fixed with 4% Perfluoroalkoxy alkane (PFA, Sigma) for 30 mins and 99.9% Methanol (Fisher) for 10 mins. Immediately after fixation, plates were filled with PBS, wrapped in parafilm, and stored at 4 C until use in cyclic immunofluorescence (CycIF).

2.4 Cyclic Immunofluorescence

Wells were washed with Odyssey blocking buffer (Fisher) for 1 h at room temperature on a rocker prior to antibody staining. Antibodies were purchased for the following proteins of interest: Alpha Smooth Muscle Actin (α -SMA), Filamentous Actin (F-Actin), Mothers Against Decapentaplegic Homolog 3 (SMAD3), Myocardin-Related Transcription Factor (MRTF), Nuclear Factor of Activated T Cells (NFAT), Nuclear Factor Kappa-light-chain-enhancer of Activated B Cells (NF- κ B), phosphorylated Extracellular Signal-Regulated Kinase (p-ERK), phosphorylated Focal Adhesion Kinase (p-FAK), phosphorylated Jun N-terminal Kinase (p-JNK), phosphorylated Protein Kinase B (p-Akt), phosphorylated p38 Mitogen-activated Protein Kinase (p-p38), and Rho-associated Protein Kinase (ROCK). Each antibody was individually optimized to determine unique staining dilutions and microscope gain, exposure, and light settings. Appendix A outlines where each antibody was purchased, Alexa Fluor conjugation, staining dilution, and microscope settings for each of the proteins of interest. The order of CycIF and protocol was determined according to previously published recommendations[22].

Four consecutive rounds of CycIF were conducted with three proteins of interest each round: (1) p-p38, NFAT, SMAD3, (2) MRTF, ROCK1, NF- κ B, (3) p-JNK, p-Akt, α -SMA, and (4) F-Actin, p-ERK, p-FAK (Figure 1). Primary and Alexa Fluor conjugated antibodies were applied and rocked overnight at 4 C. A secondary mouse-anti-rabbit IgG PE-Cy7 antibody for SMAD3, NF- κ B, α -SMAD, and p-FAK was applied for 1 h at room temperature while rocking. A Hoechst nuclear stain was rocked for ten minutes at room temperature each Cyc-IF round. All wells were washed four times with PBS between staining and imaging. Alexa Fluor light cubes GFP, TxRed, Cy7, and DAPI were used for rounds 1 and 4 of CycIF and RFP, Cy-5, Cy-7, and DAPI light cubes were used for rounds 2 and 3. The ThermoFisher Fluorescence Spectra Viewer was used to ensure minimal spectra overlap between channels[23]. An EVOS Fluorescent microscope at 10x objective was used to take ten images per well and beacons were saved to return to that position in consecutive CycIF rounds. Following each round of imaging, fluorophore inactivation was achieved by treating with 4.5% H₂O₂ (Fisher) in PBS plus 25 mM NaOH (Sigma) for 2 hs under LED lights. Inactivation was confirmed visually with the EVOS before moving on to the next round of CycIF. Wells were washed with PBS four times after destaining and before the next round of CycIF. All images were saved as 8-bit TIFF files which were imported into CellProfiler™ for post image processing[24].

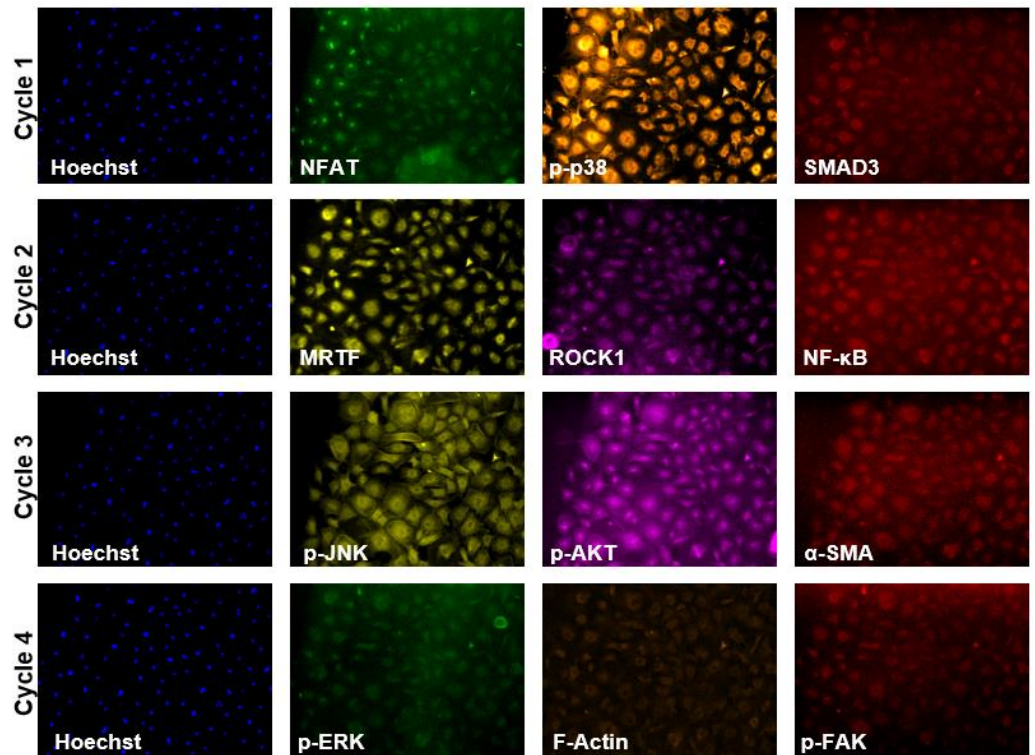


Figure 1. An example of a set of images for each of the proteins of interest for four rounds of CycIF. GFP, TxRed, and Cy7 (green, orange, and red) light cubes were used in rounds one and four. RFP, Cy5, and Cy7 (yellow, pink, and red) light cubes were used in rounds two and three. A Hoechst nuclear stain and DAPI light cube (blue) were used for all rounds.

2.5 Post Image Processing

In CellProfiler™ the lower quartile intensity background was subtracted from each image. Images from consecutive rounds of CycIF were aligned with each other to account for small changes in the field of view that occurred over multiple rounds. The Hoechst nuclear stain images were used to identify Primary Objects (the nuclei) which were then used to identify Secondary Objects (cellular outlines) (Appendix B). Morphological measurements of total cell area, nucleus area and location, and minor and major axis lengths were measured for each cell. To account for errors in the automated cell identification, an upper bound of 10000 microns² and a lower bound of 1000 microns² was set for acceptable cell areas. Integrated, mean, and median intensities were also recorded for each image channel (protein).

2.6 Statistical Analysis

In total, nearly 20,000 cells (~5,000/experimental condition) were identified across the images taken from the 8 biological replicates and used in the analysis of morphological and protein-level data. The median cell/nucleus area and elongation for each biological replicate were determined per experimental condition. To account for variability in fluorescent intensity among biological and technical replicates, normalization was conducted by dividing the channel (protein) intensity in each cell by the median of that channel intensity from all the cells on the entire plate (1 plate = 2 male and 2 female biological replicates). This allowed for the comparison of relative protein concentrations across experimental conditions. A two-way ANOVA was used to determine if there was a statistically significant ($\alpha=0.05$) difference between and within groups of sex (male vs. female) and estrogen treatment (baseline and +E2). Single-cell correlation coefficients for each protein-

protein and protein-morphology interaction were also calculated using MATLAB's built-in corrcoeff function.

3. Results

3.1. Sex-dissagregated analysis of CF morphology

Microscopic image analysis demonstrated that there was no change in cell area across experimental conditions ($p>0.05$, Figure 2.a). Likewise, cell elongation ($p>0.05$, Figure 2.b) which was calculated by determining each cell's aspect ratio (major/minor axis) was also not affected by sex or estrogen treatment. Nuclear area and aspect ratio was also observed and determined not to be dependent on sex or estrogen treatment ($p>0.05$, Figure 2.c-d). F-Actin and α -SMA's relative protein concentrations ($p>0.05$, Figure 2.e-f) also did not vary among experimental conditions, indicating that under physiological like conditions, the structure and morphological presentation of male and female CFs do not vary significantly.

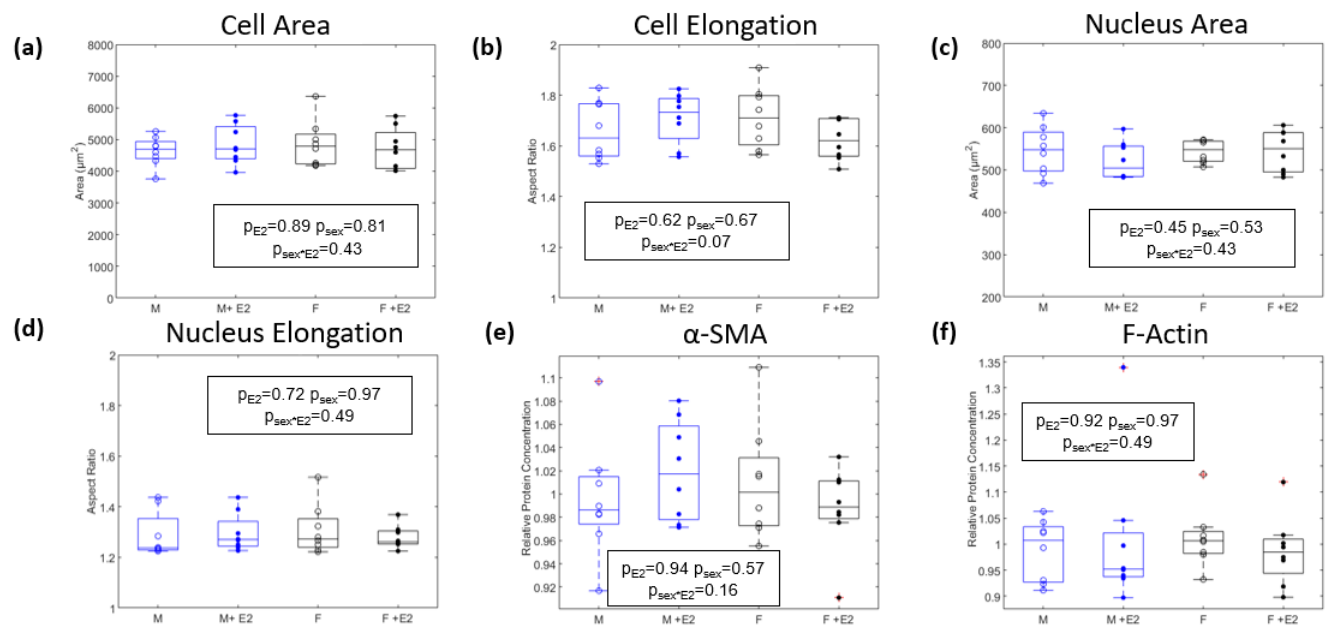


Figure 2. A two-way ANOVA was used to determine if there was any significant interaction ($\alpha=0.05$) between sex (male=blue & female=black) and estrogen treatment (baseline=open dots to represent median of biological replicates and +E2=closed dots) on morphological factors. There was no significant difference within groups or interaction between groups for total cell area and elongation (a and b) as well as nucleus area and elongation (c and d). F-Actin and α -SMA relative protein concentrations also did not significantly change between experimental conditions (e and f).

3.2. Relative concentration of fibrotic related signaling proteins

Relative protein concentration was determined by comparing normalized median cell intensities for each protein of interest. p-ERK had a statistically significant interaction between sex and E2 treatment, with the female baseline being higher than all other experimental conditions ($p<0.05$, Figure 3.a). p-p38 and ROCK1 were found to be statistically different due to sex, with male cells having higher levels of both p-p38 and ROCK1 in the baseline and E2 treated cells compared to female cells with or without E2 ($p<0.05$, Figure 3b-c). For p-FAK, there was a statistically significant down-regulation of the relative concentration of p-FAK in both male and female cells when E2 was present ($p<0.05$, Figure 3.d). There was no statistically significant change across experimental conditions for the relative protein concentrations of p-JNK and p-Akt ($p>0.05$, Figure 3e-h).

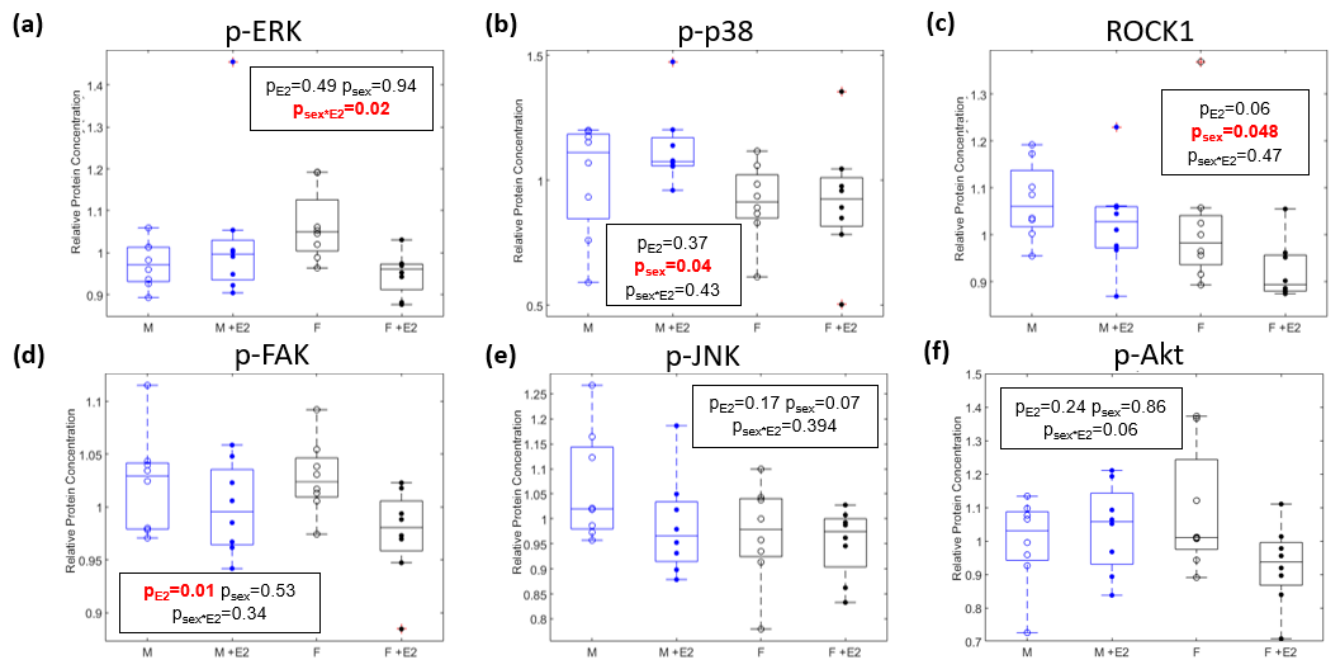


Figure 3. A two-way ANOVA was used to determine if there was any significant interaction ($\alpha=0.05$) between sex and estrogen treatment on the normalized median intensity of profibrotic proteins. For p-ERK, there was a significant interaction between sex and E2 treatment ($p<0.05$, a). The median intensity of ROCK1 and p-p38 was significantly different due to biological sex ($p<0.05$, b and c). E2 treatment caused a significant difference in median intensity for p-FAK ($p<0.05$, d). There were no significant interactions between or within groups for p-JNK, p-AKT ($p>0.05$, e and f).

3.3 Nuclear localization of mechanosensitive proteins

Many profibrotic proteins in CFs are in their most activated form when they have translocated to the nucleus allowing them to act as transcription factors to influence gene regulation. In our study, MRTF, NFAT, NF- κ B, and SMAD3 are all most activated in the nucleus and so instead of measuring their total cell intensity, the ratio of the intensity within the nucleus vs. the cytoplasm was calculated (normalized mean nuclear intensity/normalized mean cytoplasm intensity). While MRTF, NFAT, NF- κ B, and SMAD3 all had ratios greater than 1 for each experimental condition indicating that more was present in the nucleus than the cytoplasm, only the levels of NFAT were different across experimental groups ($p>0.05$, Figure 4.a-c). Male cells had NFAT levels in the nucleus that were higher than both the baseline and E2 treated female cells ($p<0.05$, Figure 4.d).

3.4 Correlation analysis of protein-protein interactions

An advantage of cyclic-IF analysis for protein quantification is that it enables single-cell measurements, which can be tested for protein-protein and protein-morphology relationships. The correlation coefficients of the normalized relative protein-protein concentrations and protein-morphology interactions were calculated along with their corresponding p-values. These data were used to create dot plots (Figure 5) which allow comparison of changes in protein-protein/protein-morphology interactions between experimental conditions. The most striking difference is that there is a much stronger correlation of protein-protein interactions for female CFs treated with estrogen (indicated by large orange and yellow dots), than male CFs treated with estrogen. Similarly, male CFs without E2 demonstrate a number of strong and significant correlations, which are dampened in the presence of E2. Female CFs experience similar correlated relationships with and without E2 treatment.

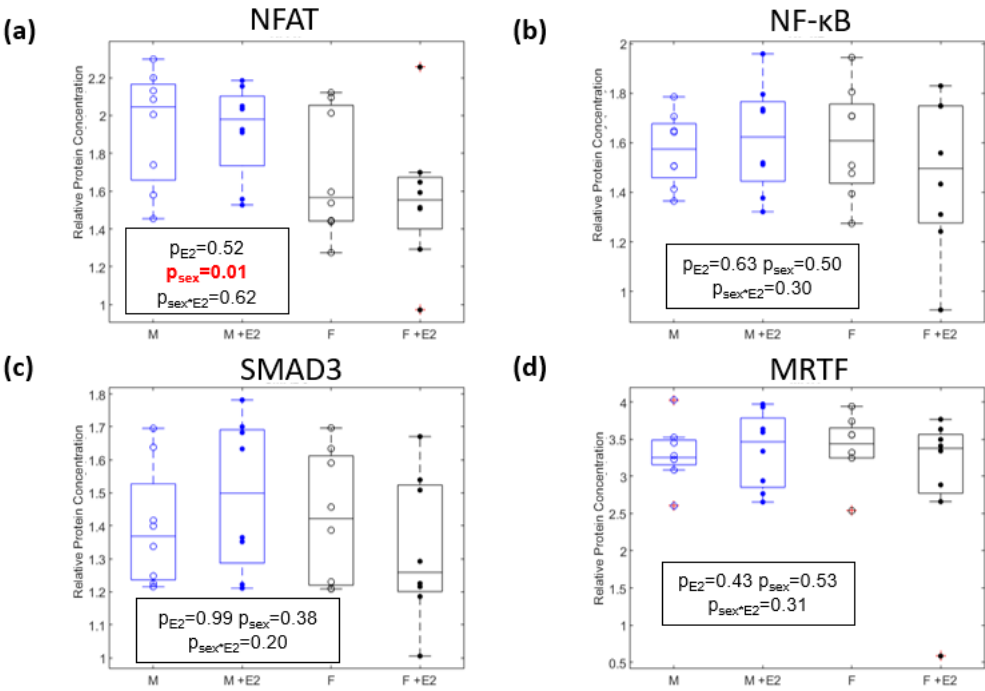


Figure 4. A two-way ANOVA was used to determine if there were any significant interactions between sex and estrogen treatment of translocation of profibrotic proteins to the nucleus. The median nucleus: cytoplasm ratio of NFAT was significantly different due to biological sex ($p<0.05$, a). There were no significant interactions between or within groups for NF-κB, SMAD3, or MRTF ($p>0.05$, b-d).

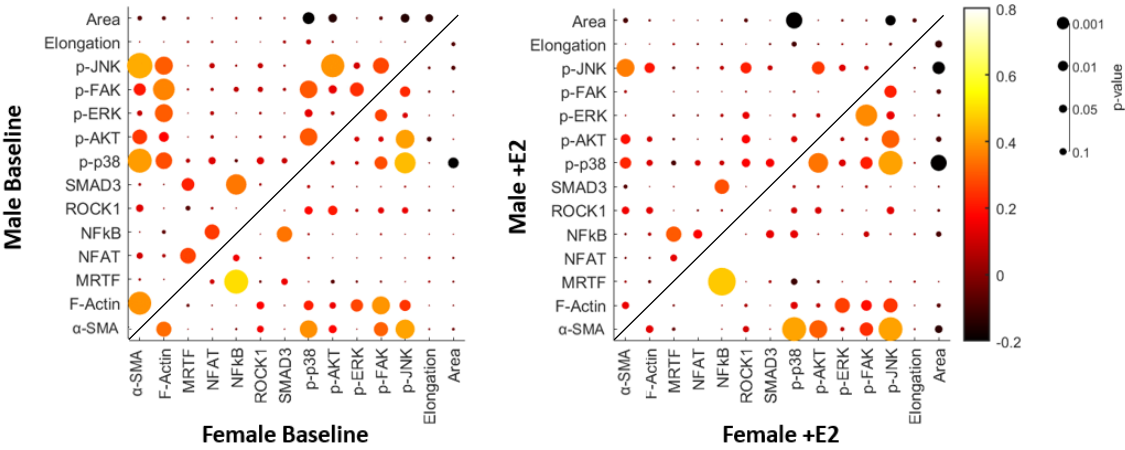


Figure 5. Dot plots of correlation coefficients and their corresponding p-values for analysis of protein-protein and protein-morphology interactions.

4. Discussion

Although many studies note the phenotypic differences between male and female cardiac fibroblasts. Very few studies have investigated if these phenotypic changes result in observable morphological differences in cell size and elongation. At a macro level, male morphology is dimorphic from that of females, with male hearts and their components including the left ventricle often being larger than female hearts from the same species[25,26]. As fibrosis progresses, CFs undergo morphological changes, elongating and taking up a larger area due to interactions with their changing microenvironment[27].

This can also result in nuclear morphologic changes mediated by LINC[19]. To fully understand the differences in how male and female CFs interact with and respond to changes in their mechanochemical environment during fibrosis progression, it is important to know if there are any noticeable morphological differences present in physiologically “healthy” environments. Our results indicate that on a stiffness which mimics physiological conditions, there are no changes in cell and nuclear morphology due to sex and estrogen treatment. This indicates that while male and female cells may phenotypically be different at an intracellular level, these changes are more likely to present biochemically rather than structurally. Our finding that there was no significant difference in α -SMA and F-Actin relative protein levels due to sex and estrogen treatment also support this theory, as both elevated α -SMA and F-Actin levels are indicative of increased cell contractility which can cause changes in cell morphology[28].

Of the 12 proteins of interest investigated, NFAT, p-p38, and ROCK1 were found to be elevated in male cells over female cells regardless of E2 treatment. Each of these proteins is typically more elevated in a profibrotic environment[19]. This indicates that even in a physiologically “healthy” environment male CFs may be more sensitive to chemical changes and prone to fibrotic behavior than female CFs. Sex disaggregated literature of the behavior of these proteins in relation to fibrosis and CFs is extremely sparse. One in vivo mice study found that female mice underwent p-38 induced ventricular hypertrophy and mortality at a slower rate than male mice[29]. More research should be done to investigate the potential intrinsic differences of these and other downstream proteins in male and female CFs to elucidate an understanding of the divergence of male and female signaling pathways. This could help with the development of sex-specific prevention and treatment methods for cardiac fibrosis.

As stated earlier, CFs are very susceptible to changes in their microenvironment. A major way they sense and translate these signals within the cell is through integrins and adhesion receptors on the cell membrane. One highly studied adhesion receptor in CFs is focal adhesion kinase (FAK) which can become activated (p-FAK) due to interactions with the extracellular matrix[27]. Inhibition of FAK has been shown to stop adverse cardiac remodeling in a multitude of studies[30,31]. Our results show that upon treatment of E2, both male and female CFs had reduced expression of p-FAK, indicating its promise as a potential regulation pathway that mimics the cardioprotective effect of estrogen. To our knowledge, there are no other studies that look at the effect of estrogen on FAK in cardiac fibroblasts. However, there are a few studies that cite how E2 treatment can actually activate FAK in breast cancer cells[32,33]. The microenvironment of a breast cancer tumor is likely much stiffer than the 8 kPa physiological like stiffness we used in our study, so it is possible that there is a complex interaction of mechanical cues and hormone signaling which affect FAK activation. FAK has many proteins downstream of it which are also considered profibrotic factors, so its pathways are a promising source of potential regulation if more research is conducted to understand its response to combined estrogen treatment and mechanical stimulus.

Not all of our proteins of interest had statistically significant differences between experimental conditions (SMAD3, NF- κ B, p-JNK, and p-Akt). This finding was slightly surprising in regards to SMAD3 and p-JNK, because of past literature that cites the ability of estrogen to downregulate SMAD3 and p-JNK activity in CFs³⁴. These contradictory findings are not out of the ordinary - a recent review of the limited research of sex differences and estrogen signaling in CFs notes a few additional discrepancies between various other peer reviewed studies as well[7]. There are many differences in experimental set up including in vivo vs. in vitro design, pooled male and female cells vs. a sex disaggregated analysis, neonatal vs. adult cells. Our study introduces a new variable to this mix: substrate stiffness. Nearly all previous in vitro studies on sex or estrogen signaling in CFs was done on TCP with an unrealistically high stiffness (>1000 fold stiffer than myocardium). It is imperative to conduct further sex/E2 focused studies within CFs controlling for individual variables before it is possible to synthesize the results from multiple studies into a broader understanding of sex-specific and estrogen-induced signaling in CFs.

The only protein of interest that had a statistically significant interaction between sex and E2 treatment was p-ERK. Baseline levels of p-ERK in female CFs were higher than all other experimental conditions, however, upon E2 treatment, female CFs had levels similar to male CFs. There was a negligible difference between male baseline and male +E2 relative protein concentrations of p-ERK. We hypothesize that this difference among experimental conditions may be related to β -Adrenergic receptors (β -ARs) which are believed to increase fibrotic activity through ERK(1/2) related pathways[34]. Many studies have observed cross-talk in β -ARs and estrogen signaling[35]. Additionally, a recent study outlined the sex dimorphic response in CFs due to β -AR stimulation[36]. As β -blockers are already an FDA-approved treatment for many cardiovascular pathologies including high blood pressure and heart failure, this connection offers a promising avenue of potential regulation of uncontrolled fibrosis that warrants further investigation.

Limitations of our study include that it was simply an in vitro monolayer culture analysis with a serum starvation used to induce the baseline lack of estrogen condition. In the future, an in vivo study with OVX mice could be used to truly mimic the changes in estrogen levels due to menopause and other differences that are difficult to capture with an in vitro platform. We also chose to use immunofluorescence so that we could capture any potential morphological and nuclear translocation of profibrotic factors intrinsic to male and female CFs with and without estrogen treatment. Our analysis indicates that there are no significant structural differences between male and female CFs on a physiologic like stiffness of 8kPa and only NFAT expressed different levels of translocation to the nucleus among experimental conditions. In the future, we would recommend that analysis is done with methods that may allow for a more robust signaling analysis such as flow cytometry, western blotting, or RNA-seq.

5. Conclusions

Our results support the existing literature that cites male and female CFs are sexually dimorphic, even under physiologically “healthy” conditions and should be treated as such when designing experiments to allow for sex-disaggregated analysis to determine how biological sex may be affecting response to treatment interventions. Much more research needs to be done to uncover the complex signaling interactions of biological sex, E2, and profibrotic signaling pathways. One way to hasten this investigation could be through the use of sex-specific computational disease models. Existing disease models such as the signaling network model of cardiac fibroblasts’ response to mechano-chemo signaling could be improved through the incorporation of biological sex and hormone pathways[37,38]. Large-scale sex-specific network modeling could greatly accelerate the pace and reduce the costs of identifying important interactions involved in the regulation of fibrosis rather than trial and error experiments alone.

Supplementary Materials: The following are available online at www.mdpi.com/xxx/s1, Figure S1: title, Table S1: title, Video S1: title.

Author Contributions: Conceptualization, K.W. and W.R.; methodology, K.W.; software, K.W.; formal analysis, K.W.; investigation, K.W.; resources, W.R.; writing—original draft preparation, K.W.; writing—review and editing, K.W. and W.R.; visualization, K.W. and W.R.; supervision, W.R.; project administration, W.R.; funding acquisition, W.R. All authors have read and agreed to the published version of the manuscript.

Funding: The authors gratefully acknowledge funding from the National Institutes of Health (HL144927, GM121342).

Institutional Review Board Statement: All animal work was approved by the Clemson University Institutional Animal Care and Use Committee, through protocol AUP 2019-048.

Informed Consent Statement: Not applicable.

Data Availability Statement: All data produced by this study will be available through the Richardson lab figshare account: <https://figshare.com/account/home/projects/121860>.

Acknowledgments: The authors gratefully acknowledge Dr. Patricia Tate for assistance in animal sacrifices and cell isolations.

Conflicts of Interest: The authors declare no conflict of interest.

References

1. Benjamin, E.J.; Muntner, P.; Alonso, A.; Bittencourt, M.S.; Callaway, C.W.; Carson, A.P.; Chamberlain, A.M.; Chang, A.R.; Cheng, S.; Das, S.R.; et al. Heart Disease and Stroke Statistics—2019 Update: A Report From the American Heart Association. *Circulation* **2019**, *139*, doi:10.1161/CIR.0000000000000659.
2. Mehta, P.A.; Cowie, M.R. Gender and Heart Failure: A Population Perspective. *Heart* **2006**, *92*, iii14–iii18, doi:10.1136/hrt.2005.070342.
3. Patrizio, M.; Marano, G. Gender Differences in Cardiac Hypertrophic Remodeling. *Annali dell'Istituto Superiore di Sanità* **2016**, doi:10.4415/ANN_16_02_14.
4. Eisenberg, E.; Di Palo, K.E.; Piña, I.L. Sex Differences in Heart Failure. *Clin Cardiol* **2018**, *41*, 211–216, doi:10.1002/clc.22917.
5. Sex and Gender Differences in Ischemic Heart Disease: Endocrine Vascular Disease Approach (EVA) Study Design | SpringerLink Available online: <https://link.springer.com/article/10.1007%2Fs12265-018-9846-5> (accessed on 14 December 2018).
6. Scott, N.S. Understanding Hormones, Menopause, and Heart Failure: Still a Work in Progress*. *Journal of the American College of Cardiology* **2017**, *69*, 2527–2529, doi:10.1016/j.jacc.2017.03.561.
7. Medzikovic, L.; Aryan, L.; Eghbali, M. Connecting Sex Differences, Estrogen Signaling, and MicroRNAs in Cardiac Fibrosis. *Journal of Molecular Medicine* **2019**, *97*, 1385–1398, doi:10.1007/s00109-019-01833-6.
8. Lobo, R.A. Hormone-Replacement Therapy: Current Thinking. *Nat Rev Endocrinol* **2017**, *13*, 220–231, doi:10.1038/nrendo.2016.164.
9. Zhao, D.; Guallar, E.; Ouyang, P.; Subramanya, V.; Vaidya, D.; Ndumele, C.E.; Lima, J.A.; Allison, M.A.; Shah, S.J.; Bertoni, A.G.; et al. Endogenous Sex Hormones and Incident Cardiovascular Disease in Post-Menopausal Women. *Journal of the American College of Cardiology* **2018**, *71*, 2555–2566, doi:10.1016/j.jacc.2018.01.083.
10. Mahmoodzadeh, S.; Dworatzek, E.; Fritschka, S.; Pham, T.H.; Regitz-Zagrosek, V. 17 β -Estradiol Inhibits Matrix Metalloproteinase-2 Transcription via MAP Kinase in Fibroblasts. *Cardiovascular Research* **2010**, *85*, 719–728, doi:10.1093/cvr/cvp350.
11. Zhou, L.; Shao, Y.; Huang, Y.; Yao, T.; Lu, L.-M. 17 β -Estradiol Inhibits Angiotensin II-Induced Collagen Synthesis of Cultured Rat Cardiac Fibroblasts via Modulating Angiotensin II Receptors. *European Journal of Pharmacology* **2007**, *567*, 186–192, doi:10.1016/j.ejphar.2007.03.047.
12. Wu, C.-H.; Liu, J.-Y.; Wu, J.-P.; Hsieh, Y.-H.; Liu, C.-J.; Hwang, J.-M.; Lee, S.-D.; Chen, L.-M.; Chang, M.-H.; Kuo, W.-W.; et al. 17 β -Estradiol Reduces Cardiac Hypertrophy Mediated through the up-Regulation of PI3K/Akt and the Suppression of Calcineurin/NF-AT3 Signaling Pathways in Rats. *Life Sciences* **2005**, *78*, 347–356, doi:10.1016/j.lfs.2005.04.077.
13. Moore-Morris, T.; Guimarães-Camboa, N.; Yutzey, K.E.; Pucéat, M.; Evans, S.M. Cardiac Fibroblasts: From Development to Heart Failure. *J Mol Med (Berl)* **2015**, *93*, 823–830, doi:10.1007/s00109-015-1314-y.
14. Dworatzek, E.; Mahmoodzadeh, S.; Schriever, C.; Kusumoto, K.; Kramer, L.; Santos, G.; Fliegner, D.; Leung, Y.-K.; Ho, S.-M.; Zimmermann, W.-H.; et al. Sex-Specific Regulation of Collagen I and III Expression by 17 β -Estradiol in Cardiac Fibroblasts: Role of Estrogen Receptors. *Cardiovascular Research* **2019**, *115*, 315–327, doi:10.1093/cvr/cvy185.
15. Chao, H.-H.; Chen, J.-J.; Chen, C.-H.; Lin, H.; Cheng, C.-F.; Lian, W.-S.; Chen, Y.-L.; Juan, S.-H.; Liu, J.-C.; Liou, J.-Y.; et al. Inhibition of Angiotensin II Induced Endothelin-1 Gene Expression by 17 β -Oestradiol in Rat Cardiac Fibroblasts. *Heart* **2005**, *91*, 664–669, doi:10.1136/hrt.2003.031898.
16. Iorga, A.; Umar, S.; Ruffenach, G.; Aryan, L.; Li, J.; Sharma, S.; Motayagheni, N.; Nadadur, R.D.; Bopassa, J.C.; Eghbali, M. Estrogen Rescues Heart Failure through Estrogen Receptor Beta Activation. *Biol Sex Differ* **2018**, *9*, doi:10.1186/s13293-018-0206-6.

17. Janmey, P.A.; Fletcher, D.A.; Reinhart-King, C.A. Stiffness Sensing by Cells. *Physiological Reviews* **2020**, *100*, 695–724, doi:10.1152/physrev.00013.2019.
18. MacLean, J.; Pasumarthi, K.B.S. Signaling Mechanisms Regulating Fibroblast Activation, Phenoconversion and Fibrosis in the Heart. *Indian J Biochem Biophys* **2014**, *51*, 476–482.
19. Herum, K.M.; Lunde, I.G.; McCulloch, A.D.; Christensen, G. The Soft- and Hard-Heartedness of Cardiac Fibroblasts: Mechanotransduction Signaling Pathways in Fibrosis of the Heart. *J Clin Med* **2017**, *6*, doi:10.3390/jcm6050053.
20. Rogers, J.D.; Holmes, J.W.; Saucerman, J.J.; Richardson, W.J. Mechano-Chemo Signaling Interactions Modulate Matrix Production by Cardiac Fibroblasts. *Matrix Biology Plus* **2021**, *10*, 100055, doi:10.1016/j.mbplus.2020.100055.
21. Fowlkes, V.; Clark, J.; Fix, C.; Law, B.A.; Morales, M.O.; Qiao, X.; Ako-Asare, K.; Goldsmith, J.G.; Carver, W.; Murray, D.B.; et al. Type II Diabetes Promotes a Myofibroblast Phenotype in Cardiac Fibroblasts. *Life Sciences* **2013**, *92*, 669–676, doi:10.1016/j.lfs.2013.01.003.
22. Lin, J.; Fallahi-Sichani, M.; Chen, J.; Sorger, P.K. Cyclic Immunofluorescence (CycIF), A Highly Multiplexed Method for Single-cell Imaging. *Current Protocols in Chemical Biology* **2016**, *8*, 251–264, doi:10.1002/cpch.14.
23. Fluorescence SpectraViewer Available online: <https://www.thermofisher.com/order/fluorescence-spectraviewer> (accessed on 2 July 2021).
24. McQuin, C.; Goodman, A.; Chernyshev, V.; Kametsky, L.; Cimini, B.A.; Karhohs, K.W.; Doan, M.; Ding, L.; Rafelski, S.M.; Thirstrup, D.; et al. CellProfiler 3.0: Next-Generation Image Processing for Biology. *PLOS Biology* **2018**, *16*, e2005970, doi:10.1371/journal.pbio.2005970.
25. de Simone, G.; Devereux, R.B.; Daniels, S.R.; Meyer, R.A. Gender Differences in Left Ventricular Growth. *Hypertension* **1995**, *26*, 979–983, doi:10.1161/01.HYP.26.6.979.
26. Schaible, T.F.; Scheuer, J. Comparison of Heart Function in Male and Female Rats. *Basic Res Cardiol* **1984**, *79*, 402–412, doi:10.1007/BF01908140.
27. Herum, K.M.; Choppe, J.; Kumar, A.; Engler, A.J.; McCulloch, A.D. Mechanical Regulation of Cardiac Fibroblast Profibrotic Phenotypes. *Mol Biol Cell* **2017**, *28*, 1871–1882, doi:10.1091/mbc.E17-01-0014.
28. Hinz, B.; Celetta, G.; Tomasek, J.J.; Gabbiani, G.; Chaponnier, C. Alpha-Smooth Muscle Actin Expression Upregulates Fibroblast Contractile Activity. *Mol Biol Cell* **2001**, *12*, 2730–2741.
29. Dash, R.; Schmidt, A.G.; Pathak, A.; Gerst, M.J.; Biniakiewicz, D.; Kadambi, V.J.; Hoit, B.D.; Abraham, W.T.; Kranias, E.G. Differential Regulation of P38 Mitogen-Activated Protein Kinase Mediates Gender-Dependent Catecholamine-Induced Hypertrophy. *Cardiovascular Research* **2003**, *57*, 704–714, doi:10.1016/S0008-6363(02)00772-1.
30. Zhang, J.; Fan, G.; Zhao, H.; Wang, Z.; Li, F.; Zhang, P.; Zhang, J.; Wang, X.; Wang, W. Targeted Inhibition of Focal Adhesion Kinase Attenuates Cardiac Fibrosis and Preserves Heart Function in Adverse Cardiac Remodeling. *Sci Rep* **2017**, *7*, 43146, doi:10.1038/srep43146.
31. Fan, G.-P.; Wang, W.; Zhao, H.; Cai, L.; Zhang, P.-D.; Yang, Z.-H.; Zhang, J.; Wang, X. Pharmacological Inhibition of Focal Adhesion Kinase Attenuates Cardiac Fibrosis in Mice Cardiac Fibroblast and Post-Myocardial-Infarction Models. *CPB* **2015**, *37*, 515–526, doi:10.1159/000430373.
32. Rigracciolo, D.C.; Santolla, M.F.; Lappano, R.; Vivacqua, A.; Cirillo, F.; Galli, G.R.; Talia, M.; Muglia, L.; Pellegrino, M.; Nohata, N.; et al. Focal Adhesion Kinase (FAK) Activation by Estrogens Involves GPER in Triple-Negative Breast Cancer Cells. *J Exp Clin Cancer Res* **2019**, *38*, 58, doi:10.1186/s13046-019-1056-8.
33. Tsai, C.-L.; Wu, H.-M.; Lin, C.-Y.; Lin, Y.-J.; Chao, A.; Wang, T.-H.; Hsueh, S.; Lai, C.-H.; Wang, H.-S. Estradiol and Tamoxifen Induce Cell Migration through GPR30 and Activation of Focal Adhesion Kinase (FAK) in Endometrial Cancers with Low or without Nuclear Estrogen Receptor α (ER α). *PLOS ONE* **2013**, *8*, e72999, doi:10.1371/journal.pone.0072999.
34. Tanner, M.A.; Thomas, T.P.; Maitz, C.A.; Grisanti, L.A. B2-Adrenergic Receptors Increase Cardiac Fibroblast Proliferation Through the Gas/ERK1/2-Dependent Secretion of Interleukin-6. *Int J Mol Sci* **2020**, *21*, E8507, doi:10.3390/ijms21228507.

-
35. Matarrese, P.; Maccari, S.; Vona, R.; Gambardella, L.; Stati, T.; Marano, G. Role of β -Adrenergic Receptors and Estrogen in Cardiac Repair after Myocardial Infarction: An Overview. *International Journal of Molecular Sciences* **2021**, *22*, 8957, doi:10.3390/ijms22168957.
 36. Peter, A.K.; Walker, C.J.; Ceccato, T.; Trexler, C.L.; Ozeroff, C.D.; Lugo, K.R.; Perry, A.R.; Anseth, K.S.; Leinwand, L.A. Cardiac Fibroblasts Mediate a Sexually Dimorphic Fibrotic Response to β -Adrenergic Stimulation. *Journal of the American Heart Association* **2021**, *10*, e018876, doi:10.1161/JAHA.120.018876.
 37. Zeigler, A.C.; Richardson, W.J.; Holmes, J.W.; Saucerman, J.J. Computational Modeling of Cardiac Fibroblasts and Fibrosis. *Journal of Molecular and Cellular Cardiology* **2016**, *93*, 73–83, doi:10.1016/j.yjmcc.2015.11.020.
 38. Rogers, J.D.; Richardson, W.J. *Fibroblast Mechanotransduction Network Predicts Targets for Mechano-Adaptive Infarct Therapies*; 2020; p. 2020.08.13.250001;